Effective masses of holes at GaAs-AlGaAs heterojunctions

D. A. Broido and L. J. Sham
Department of Physics, University of California, San Diego, La Jolla, California 92093
(Received 6 August 1984)

The spin-split hole subband structure for a GaAs p-channel inversion layer is calculated. From it, density-of-states masses and cyclotron masses as a function of magnetic field are extracted. Results indicate significant discrepancies between calculated and measured masses. Many-body effects on the effective mass may be important.

I. INTRODUCTION

p-channel inversion layers have been studied extensively in Si metal-oxide semiconductor field-effect transistors (MOSFET'S).[1,2] With the advent of modulation doping, it has become possible to form p-channel inversion layers at a GaAs-AlGaAs heterojunction.[3] Since an inversion layer is characterized by the motion of carriers parallel to the interface it is desirable to have a description of the subband structure. In GaAs, the interaction between the conduction and valence bands is small because of the large energy gap, E_g ($E_g \simeq 1.5$ eV). As a result, in an n-channel GaAs inversion layer the motion parallel to the interface is hardly affected by the quantization of the perpendicular motion. In a p-channel GaAs inversion layer, however, this is not the case. The degeneracy of the valence bands and the surface electric field combine to couple strongly the parallel and perpendicular motion. The hole subbands are then highly nonparabolic.

An additional property predicted theoretically for p-channel Si inversion layers is the lifting of the twofold spin degeneracy of the holes produced by the interplay of the lack of inversion symmetry of the interface potential and the spin-orbit coupling.[1,2] As a result, the two-dimensional hole levels consist of two distinct subbands each characterized by its own effective mass. In GaAs, which has a larger spin-orbit coupling, this effect is expected to be more prominent than in Si. Indeed, it has been observed in recent magnetotransport and cyclotron resonance measurements on a p-channel inversion layer at a GaAs-AlGaAs heterojunction which showed the existence of two cyclotron masses of $0.60m_0$ and $0.38m_0$.[4] This paper addresses the results of Ref. 4.

We present a simple-model calculation of the GaAs hole subband structure, the density-of-states (DOS) masses, and the cyclotron masses as a function of magnetic field. Section II lists the approximations made. In Sec. III, an outline of the calculation and results for the case of zero magnetic field are given. In Sec. IV, the same is done for the finite-field case. Section V is devoted to discussion and conclusions.

II. THEORY

Our calculations are performed for both zero and finite magnetic field, B, at zero temperature. We make the following simplifying assumptions:

(a) The 4×4 Luttinger $\vec{k}\cdot\vec{p}$ Hamiltonian[5] adequately describes the band structure of the upper four valence bands around Γ_8. The split-off bands at Γ_7 lie at an energy 340 meV below Γ_8 so they are neglected.

(b) The mole fraction of Al in $Al_xGa_{1-x}As$ is large ($x=0.5$) so that the energy step, ΔE_v, between the valence-band edges of GaAs and $Al_xGa_{1-x}As$ is also large ($\Delta E_v \sim 100$—400 meV).[6,7] Since the relevant energies in the problem are about 10 meV, ΔE_v is assumed infinite. The total wave function then vanishes at the interface.

(c) Linear k terms[8] caused by the lack of inversion symmetry of the zinc-blende structure are neglected. An estimate of the resulting error is given in Sec. V.

(d) The Hartree approximation is used. Many-body effects such as exchange and correlation are not included.

III. $B=0$ CASE

For zero magnetic field, the 4×4 Luttinger Hamiltonian for the light and heavy hole bands around Γ_8, including the linear k terms T and T', is (in atomic units with hole energy counted as positive)

$$H_0(k_x,k_y,k_z)=\begin{pmatrix} P+Q & R-T' & -S+\frac{1}{\sqrt{3}}T^* & T \\ R^*-T' & P-Q & -T & S+\frac{1}{\sqrt{3}}T^* \\ -S^*+\frac{1}{\sqrt{3}}T & -T^* & P-Q & R+T' \\ T^* & S^*+\frac{1}{\sqrt{3}}T & R^*+T' & P+Q \end{pmatrix}, \tag{1}$$

where

$$P=\frac{\gamma_1}{2}(k_z^2+k^2),\quad Q=\frac{\gamma_2}{2}(-2k_z^2+k^2)\ ,$$
$$R=-\frac{\sqrt{3}}{2}\bar{\gamma}k_-^2+\frac{\sqrt{3}}{2}\mu k_+^2,\quad S=\sqrt{3}\gamma_3 k_z k_-\ ,$$
$$T=-\beta k_-,\quad T'=-\frac{2}{\sqrt{3}}\beta k_z\ , \tag{2}$$
$$k_\pm=k_x\pm ik_y,\quad k^2=k_x^2+k_y^2\ ,$$
$$\bar{\gamma}=\tfrac{1}{2}(\gamma_2+\gamma_3),\quad \mu=\tfrac{1}{2}(\gamma_3-\gamma_2)\ .$$

In T and T', $\beta\equiv-(\sqrt{3}/2)C$ where the constant C is defined by Dresselhaus.[8] We take $\beta=0$ for now and discuss the case $\beta\neq 0$ in Sec. V.

The Luttinger parameters, γ_1, γ_2, and γ_3, are taken from Ref. 9: $\gamma_1=6.85$, $\gamma_2=2.1$, and $\gamma_3=2.9$. A unitary transformation block diagonalizes the Hamiltonian H_0 into two 2×2 blocks:

$$H_0'=\begin{bmatrix}H^U & 0\\ 0 & H^L\end{bmatrix}, \tag{3}$$

where the upper and lower blocks, H^U and H^L, are given by

$$H^\sigma=\begin{bmatrix}P\pm Q & \tilde{R}\\ \tilde{R}^* & P\mp Q\end{bmatrix},\quad \tilde{R}=|R|-i|S|\ , \tag{4}$$

where $\sigma=U\ (L)$ refers to the upper (lower) $\pm$ signs. The double degeneracy of the heavy and light hole bands without the linear k terms is now apparent. The original basis set and transformation are given in the Appendix.

We choose the z direction to be perpendicular to the interface. Incorporating the slowly varying interface potential within the effective-mass approximation (EMA) results in an effective Hamiltonian for the envelope functions:

$$H_{\text{eff}}=H_0'(k_x,k_y,\hat{k}_z)+V(z)\ , \tag{5}$$

where $\hat{k}_z$ stands for the operator $(1/i)\partial/\partial z$. In a first approximation, we neglect the band warping. This is done by letting μ be 0 in the element R of Eq. (1), a simplification which produces only a small change in H_0 for finite k_x,k_y and no change for $k_x=k_y=0$. Then, H_{eff} depends on k, the magnitude of vector (k_x,k_y). The upper- and lower-block envelope functions, $\{\psi_{i,k}^\sigma(\vec{r})\}$, satisfy

$$\sum_{j=1}^{2}\left[H_{ij}^\sigma(k,\hat{k}_z)+V(z)\delta_{ij}\right]\psi_{j,k}^\sigma(\vec{r})=\epsilon^\sigma(k)\psi_{i,k}^\sigma(\vec{r})\ . \tag{6}$$

For the upper (lower) block, $i,j=1$ refer to the heavy (light) hole solutions and $i,j=2$ refer to the light (heavy) hole solutions.

The potential $V(z)$ in the Hartree approximation is taken to consist of two parts:

$$V(z)=V_{\text{inv}}(z)+V_{\text{dep}}(z)\ , \tag{7}$$

where $V_{\text{inv}}(z)$ is the potential produced by the mobile holes which form the inversion layer and $V_{\text{dep}}(z)$ is the potential created by the fixed depletion-layer charges. The inversion-layer density is taken from Ref. 4 to be $n_{\text{inv}}=5\times 10^{11}\ \text{cm}^{-2}$, while the depletion-layer density is $N_{\text{dep}}=10^{15}\ \text{cm}^{-3}$ from Ref. 3. $V(z)$ is determined self-consistently from Eq. (6) and Poisson's equation:

$$\frac{d^2V}{dz^2}=\frac{4\pi e^2}{\epsilon_s}\left[\sum_{\sigma,j,k}|\psi_{j,k}^\sigma(\vec{r})|^2+N_{\text{dep}}\right]\ , \tag{8}$$

where $\sigma=U,L$, $J=1,2$, $\epsilon_s=13.1$. (ϵ_s is the static dielectric constant for GaAs.)

Our calculation is variational in nature and consists of a $k=0$, and a finite-k analysis. We first observe that for $k=0$, H^U and H^L become diagonal with elements.

$$H_h=-\tfrac{1}{2}(\gamma_1-2\gamma_2)\frac{d^2}{dz^2}+V(z)\ ,$$
$$H_l=-\tfrac{1}{2}(\gamma_1+2\gamma_2)\frac{d^2}{dz^2}+V(z) \tag{9}$$

that yield an infinite set of doubly degenerate heavy and light hole subband energies. We therefore construct the envelope functions for finite k as

$$\psi_{h,k}^\sigma(\vec{r})=e^{i\vec{k}\cdot\vec{\rho}}\sum_{j=0}^{\infty}A_{jh}^\sigma(k)\psi_{jh}(z)\ ,$$
$$\psi_{l,k}^\sigma(\vec{r})=e^{i\vec{k}\cdot\vec{\rho}}\sum_{j=0}^{\infty}A_{jl}^\sigma(k)\psi_{jl}(z)\ , \tag{10}$$

where j is the subband index, while h and l refer to heavy and light holes. The z-dependent functions, $\psi_{jh}(z)$ and $\psi_{jl}(z)$, determine the $k=0$ energies:

$$\epsilon_{jh}(0)=\langle\psi_{jh}|H_h|\psi_{jh}\rangle\ ,$$
$$\epsilon_{jl}(0)=\langle\psi_{jl}|H_l|\psi_{jl}\rangle\ . \tag{11}$$

We take

$$\psi_{0h}(z)=\frac{2}{a_h^{3/2}}ze^{-z/a_h},\quad \psi_{0l}(z)=\frac{2}{a_l^{3/2}}ze^{-z/a_l}$$

for the lowest heavy and light hole levels and construct higher-level wave functions orthogonal to all lower ones. $\epsilon_{0h}(0)$ and $\epsilon_{0l}(0)$ are minimized with respect to a_h and a_l. The z-dependent part of the envelope functions is now completely determined. For finite k we minimize the subband energy $\epsilon^\sigma(k)$, of Eq. (6), with respect to the coefficients in the expansions of Eq. (10). For the additional z dependence introduced in this case, we define

$$s_{ij}=\langle\psi_{ih}|\psi_{jl}\rangle\ \text{and}\ K_{ij}=\left\langle\psi_{ih}\left|\frac{d}{dz}\right|\psi_{jl}\right\rangle\ .$$

Solution of the resulting eigenvalue matrix gives the subband structure. These minimizations are performed on each iteration of the potential until self-consistency is achieved. For small k, only the lowest terms in the wave-function expansions contribute significantly. We therefore retain only the first two terms in $\psi_{h,k}^\sigma(\vec{r})$, $\psi_{l,k}^\sigma(\vec{r})$ ($\sigma=U,L$) corresponding to the lowest two heavy and lowest two light hole levels. The resulting self-consistent potential along with these four levels and the Fermi level

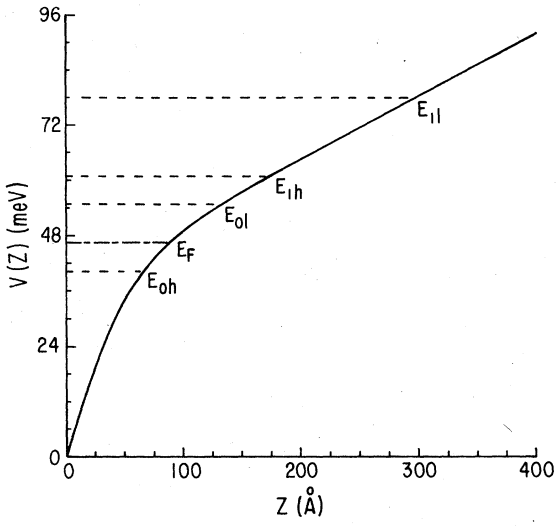

FIG. 1. Self-consistent potential, lowest two heavy and lowest two light hole levels, and Fermi level.

are plotted in Fig. 1. Note that for $n_{\rm inv}=5\times10^{11}$ cm^{-2}, only the lowest hole level is occupied. Figure 2 shows the GaAs subband structure for the lowest heavy and light hole levels. The large subband splitting for finite k is a consequence of the lifting of the spin degeneracy implicit in the bulk Hamiltonian, Eq. (3), which arises from the sign difference of the S terms of matrix equation (1) and the fact that $V(-z)\neq V(z)$. This splitting gives rise to two distinct DOS effective masses for the $\mu=0$ case:

$$\frac{m^*_{h\pm}}{m_0}=\frac{\hbar^2}{m_0}\left[\frac{1}{k}\frac{d\epsilon_{h\pm}}{dk}\right]^{-1}\Bigg|_{k_{F_\pm}}, \tag{12}$$

which yield the values shown in the top line of Table I.

By including the warping term, $\mu\neq0$, but keeping the self-consistent potential derived for $\mu=0$, we obtain the energy contours shown in Fig. 3. The Fermi energy is determined from the requirement that the number of states available within the areas enclosed by the two surfaces, $A_+(\epsilon_F)$ and $A_-(\epsilon_F)$, be equal to the total concentration

$$n_{\rm inv}=\frac{1}{4\pi^2}[A_+(\epsilon_F)+A_-(\epsilon_F)]\ . \tag{13}$$

The classical cyclotron masses derived from

$$m^*_{h\pm}=\frac{\hbar^2}{2\pi}\frac{dA_\pm}{d\epsilon}\Bigg|_{\epsilon_F} \tag{14}$$

are given in the bottom line of Table I. They are the same as DOS masses. The significant warping of the heavier mass branch produces a noticeable change in the heavier mass. The lighter mass remains unchanged since its branch is still virtually isotropic.

TABLE I. DOS masses for $\mu=0$ and 0.4.

μ	m^*_{h+}/m_0	m^*_{h-}/m_0
0	0.46	0.12
0.4	0.50	0.12
Experiment (Ref. 4)	0.60	0.38

IV. $B\neq0$ CASE

In the presence of an external magnetic field B in the z direction, the effective Hamiltonian $H_{\rm eff}$ neglecting linear k terms is obtained from Eq. (1) by replacing the components of the wave vector by their operator forms,

$$k_\alpha\rightarrow\hat{k}_\alpha=\frac{1}{i}\frac{\partial}{\partial x_\alpha}+\frac{e}{c\hbar}A_\alpha\ ,$$

and by including the κ terms[5,9] which represent the in-

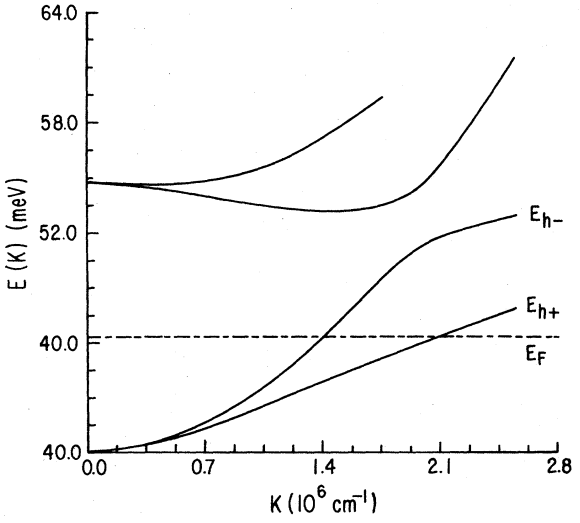

FIG. 2. Lowest heavy and lowest light hole subbands.

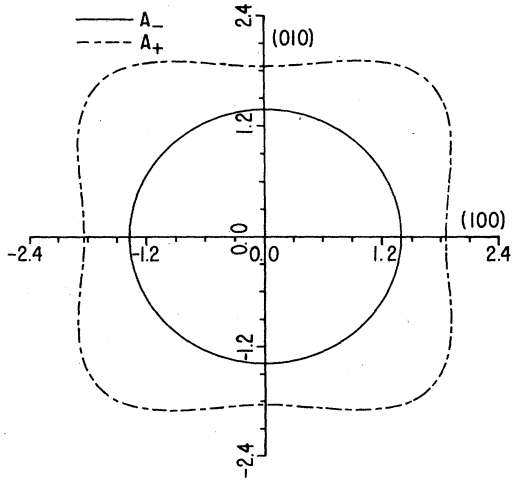

FIG. 3. Constant energy contours for the split heavy hole subbands.

teraction of the electron's spin magnetic moment with the external magnetic field. $\{A_\alpha\}$ are the components of the vector potential of the magnetic field. We choose the Landau gauge $\vec{A}=(-By,0,0)$. Writing $H_{\rm eff}$ in terms of the creation and destruction operators,

$$a^\dagger=\frac{R_c}{\sqrt{2}}k_+,\quad a=\frac{R_c}{\sqrt{2}}k_-,\quad R_c=\left[\frac{\hbar c}{eB}\right]^{1/2},\quad N=a^\dagger a\ , \tag{15}$$

and again making the no-warping approximation, $\mu\to 0$ leads to solutions which can be written in terms of the harmonic-oscillator functions, $u_n(x,y)$:

$$\begin{bmatrix}\psi_{1,n}(z) & u_{n-2}\\ \psi_{2,n}(z) & u_n\\ \psi_{3,n}(z) & u_{n-1}\\ \psi_{4,n}(z) & u_{n+1}\end{bmatrix}, \tag{16}$$

where the $\{\psi_{i,n}\}$ are expanded in terms of the z-dependent functions in Eq. (10). The u_n satisfy $a^\dagger u_n=(n+1)^{1/2}u_{n+1}$, $au_n=n^{1/2}u_{n-1}$, and $Nu_n=nu_n$. The procedure followed from this point is analogous to that for the $B=0$ case. For the four-level model, an 8×8 determinantal equation is obtained for $n\geq 2$. For $n=1$, we must set $\psi_{1,n}=0$ which leaves a 6×6 equation. For $n=0$, we choose $\psi_{1,n}=\psi_{3,n}=0$ which gives a 4×4 equation, while for $n=-1$, we take $\psi_{1,n}=\psi_{2,n}=\psi_{3,n}=0$ for which a 2×2 equation results. The solutions give the Landau levels as a function of magnetic field plotted in Fig. 4. The curvature of the levels is caused by the valence-band coupling and the strong surface electric field. The splitting of ϵ_{h+} and ϵ_{h-} levels is primarily due again to the lack of inversion symmetry and large spin-orbit coupling. The cyclotron masses are calculated from the energy difference between the highest occupied and lowest unoccupied levels subject to the conditions $\Delta n=\pm 1$:

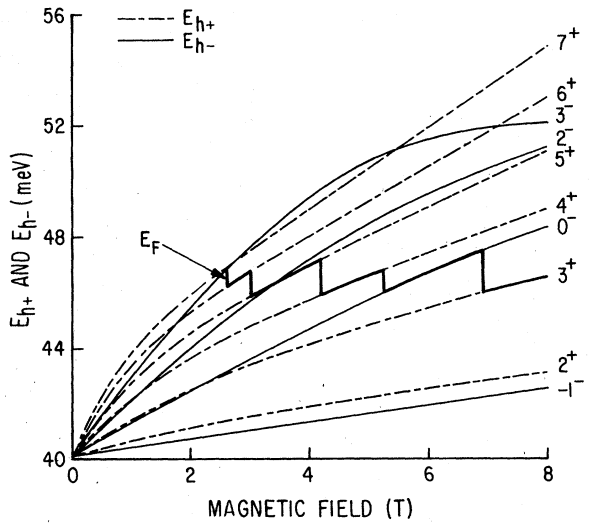

FIG. 4. Landau levels vs B for lowest heavy hole subbands.

TABLE II. Cyclotron masses as a function of magnetic field.

B (T)	m^*_{h+}/m_0	m^*_{h-}/m_0
0	0.46	0.12
2	0.45	0.16
4	0.44	0.18
6	0.35	0.24
8	0.38	0.16

$$h\omega_c^\pm(B)=\epsilon_{h\pm}^{n+1}(B)-\epsilon_{h\pm}^n(B),\quad \omega_c^\pm=\frac{eB}{m^*_{h\pm}c}\ . \tag{17}$$

The level degeneracy ζ is approximated by that for parabolic band structure: $\zeta=eB/hc$. The cyclotron masses are tabulated in Table II. Note that the masses are B-field dependent, and that they converge to the DOS masses in the low-B-field limit.

V. DISCUSSION

Comparison of the zero-field masses with the ones measured by cyclotron resonance[4] shows reasonable agreement for the heavier mass but significant disagreement for the lighter mass. Although our calculation was not carried out to convergence, we did test the sensitivity of the masses to the number of terms included in the envelope-function expansion of Eq. (10). With only the lowest-order terms for $\psi^\sigma_{h,k}$ and $\psi^\sigma_{l,k}$ retained (two-level model), the $\mu=0$ DOS masses were $m^*_{h+}=0.38m_0$, $m^*_{h-}=0.11m_0$; with the lowest two terms in $\psi^\sigma_{h,k}$ and lowest term in $\psi^\sigma_{l,k}$ (three-level model), the masses were $m^*_{h+}=0.43m_0, m^*_{h-}=0.11m_0$. Inclusion of higher-order terms, then, produces a much more pronounced increase in the heavier mass than in its lighter counterpart, suggesting that convergence of the calculation would still leave the lighter mass far too low.

When the linear k terms, T and T', are included in Eq. (1), an increase in the splitting of the subbands is induced with a consequent change in the effective masses. Brillouin scattering experiments were unable to detect the linear k splitting in GaAs,[10] but have given a value of $C=20.6$ meV-Å in CdTe.[11] We take this value as a generous upper bound for GaAs. This results in changes of only about 10% in the larger mass and 5% in the smaller one. Our neglect of T and T' is therefore justified.

The field dependence of the cyclotron masses in Table II is a consequence of the nonlinearity of the Landau levels which in turn results from the nonparabolicity of the subbands. The sharp curvature of the E_{h-} levels of Fig. 4 produce a pronounced field dependence for m_{h-} while the more linear E_{h+} levels lead to a less field dependent m_{h+}. The measured cyclotron masses[4] show far less field dependence and are larger than the calculated masses. More recent de Haas–Shubnikov measurements[12] did reveal a B-dependent lighter mass. However, its magnitude of about 0.3 below 1 T is larger than ours.

In our calculation, we have neglected many-body effects beyond the Hartree approximation. We now consider the importance of these effects on a two-dimensional system

of holes. Kohn[13] has shown that in a two-dimensional system with translational symmetry, a perturbing microwave E field only connects eigenstates of the Hamiltonian whose energies are separated by $\hbar\omega_c$. The cyclotron mass is consequently unaffected by the electron interaction. We carry out a similar analysis using the effective Hamiltonian of Sec. IV, with the Coulomb interaction included in the EMA. In this case, the microwave perturbation is not restricted to connect only eigenstates with energies separated by $\hbar\omega_c$ because the strong interaction between bands breaks the translational symmetry. Kohn's theorem is then not applicable for holes. This result, coupled with the large-r_s value ($r_s \sim 5$) for holes at 5×10^{11} cm^{-2}, indicates the strong contribution of the hole-hole interaction to the effective masses. We intend to investigate this effect.

ACKNOWLEDGMENTS

This work was supported in part by the National Science Foundation Grant No. DMR80-018440. L.J.S. also acknowledges with gratitude support from the Guggenheim Foundation.

APPENDIX

The basis set for the matrix, Eq. (1), is the (J,m_J) basis for $J=\frac{3}{2}$:

$$u_1 = |\tfrac{3}{3},\tfrac{3}{2}\rangle = \frac{-1}{\sqrt{2}}|(x+iy)\uparrow\rangle ,$$

$$u_2 = |\tfrac{3}{2},-\tfrac{1}{2}\rangle = \frac{1}{\sqrt{6}}|(x-iy)\uparrow\rangle + (\tfrac{2}{3})^{1/2}|z\downarrow\rangle ,$$

$$u_3 = |\tfrac{3}{2},\tfrac{1}{2}\rangle = \frac{-1}{\sqrt{6}}|(x+iy)\downarrow\rangle + (\tfrac{2}{3})^{1/2}|z\uparrow\rangle ,$$

$$u_4 = |\tfrac{3}{2},-\tfrac{3}{2}\rangle = \frac{1}{\sqrt{6}}|(x-iy)\downarrow\rangle .$$

The unitary transformation is

$$U = \begin{bmatrix} \frac{1}{\sqrt{2}}e^{-i\phi} & 0 & 0 & -\frac{1}{\sqrt{2}}e^{i\phi} \\ 0 & \frac{1}{\sqrt{2}}e^{-i\eta} & -\frac{1}{\sqrt{2}}e^{i\eta} & 0 \\ 0 & \frac{1}{\sqrt{2}}e^{-i\eta} & \frac{1}{\sqrt{2}}e^{i\eta} & 0 \\ \frac{1}{\sqrt{2}}e^{-i\phi} & 0 & 0 & \frac{1}{\sqrt{2}}e^{i\phi} \end{bmatrix} .$$

ϕ and η are chosen so that $H_0' \equiv UH_0U^\dagger$ is block diagonalized.

[1]E. Banghert, K. von Klitzing, and G. Landwehr, in *Proceedings of the Twelfth International Conference on the Physics of Semiconductors, Stuttgart, 1974,* edited by M. H. Pilkuhn (Teubner, Stuttgart, 1974), p. 714.
[2]F. J. Ohkawa and Y. Uemura, Suppl. Prog. Theor. Phys. Suppl. **57**, 164 (1975).
[3]H. L. Stormer and W. T. Tsang, Appl. Phys. Lett. **36**, 126 (1980).
[4]H. L. Stormer, A. Chang, Z. Schlesinger, D. C. Tsui, A. C. Gossard, and W. Wiegmann, Phys. Rev. Lett. **51**, 126 (1983).
[5]J. M. Luttinger, Phys. Rev. **102**, 1030 (1956).
[6]R. Dingle, Festkoerperprobleme **15**, 21 (1975).
[7]R. C. Miller, D. A. Kleinman, and A. C. Gossard, Phys. Rev. B **29**, 7085 (1984).
[8]G. Dresselhaus, Phys. Rev. **100**, 580 (1955).
[9]K. Hess, D. Bimberg, N. O. Lipari, J. U. Fischbach, and M. Altarelli, in *Proceedings of the XIII International Conference on the Physics of Semiconductors, Rome, 1976,* edited by F. G. Fumi (North-Holland, Amsterdam, 1976), p. 142.
[10]R. Sooryakumar and P. E. Simmonds, Solid State Commun. **42**, 287 (1982).
[11]R. Sooryakumar and M. Cardona, Solid State Commun. **48**, 581 (1983).
[12]J. Eisenstein and H. L. Stormer, private communication.
[13]W. Kohn, Phys. Rev. **123**, 1242 (1962).